Journal of Applied Polymer Science

Physical Gels of [BMIM][BF_4] by *N-tert*-Butylacrylamide/Ethylene Oxide Based Triblock Copolymer Self-Assembly: Synthesis, Thermomechanical, and Conducting Properties

Nitin Sharma,[1] Rubinder Kaur Lakhman,[1] Yuxiang Zhou,[2] Rajeswari M. Kasi[1,2]
[1]Polymer Program, Institute of Materials Science, University of Connecticut, Storrs, Connecticut-06269
[2]Chemistry Department, University of Connecticut, Storrs, Connecticut-06269
Correspondence to: R. M. Kasi (E-mail: kasi@ims.uconn.edu)

ABSTRACT: We report a strategy to prepare and characterize mechanically robust, transparent, thermoreversible physical gels of an ionic liquid 1-butyl-3-methylimidazolium tetrafluoroborate, [BMIM][BF_4], to harness its good ionic conductivity and electrolytic properties for solid-state electrolyte and lithium ion battery applications. Physical gels are prepared using a triblock copolymer comprising central polyethylene oxide block that is soluble in [BMIM][BF_4] and the end blocks, poly(*N-tert*-butylacrylamide), that are insoluble in [BMIM][BF_4]. Transparent, strong, physical ion-gels with significant mechanical strength can be formed at low concentration of the triblock copolymer (~5 wt %), unlike previous reports in which chemical gels of [BMIM][BF_4] are obtained at very high polymer concentration. Our gels are thermoreversible and thermally stable, showing 1–4% weight loss up to 200°C in air. Gelation behavior, mechanical properties, and ionic conductivity of these ion-gels can be easily tuned by varying the concentration or *N-tert*-butylacrylamide block length in the triblock copolymer. These new non-volatile, reprocessable, mechanically robust, [BMIM][BF_4]-based physical ion-gels obtained from a simple and convenient preparation method are promising materials for solid-state electrolyte applications. © 2012 Wiley Periodicals, Inc. J. Appl. Polym. Sci. 128: 3982–3992, 2013

KEYWORDS: gels; ionic liquids; rheology; self-assembly; copolymers

Received 8 July 2012; accepted 22 September 2012; published online 16 October 2012
DOI: 10.1002/app.38629

INTRODUCTION

The development of solid polymer electrolytes for device applications with high ionic conductivities is essentially driven by key disadvantages of liquid electrolytes, including but not limited to, flammability, leakage, toxicity, short-circuiting, and undesirable detrimental side-reactions.[1,2] The use of polymer electrolytes not only overcomes the problems of liquid electrolytes, but also offers other features such as shape versatility and flexibility in design (thickness, area, and shape).[3–5] Conventional electrolytes in this category consist of solid solutions of electrolyte salts in polyethylene oxide (PEO)-based polymers. However, the performance in polymer electrolytes is often limited by low ionic conductivity.[6] Several studies have shown that lower ion mobility in these polymeric electrolytes arises due to segmental and chain mobility of the polymer which is dictated by high glass transition temperature (T_g) and crystallinity.[7] This is a significant drawback in their utilization as solid electrolytes and as a result research efforts are directed to increase the conductivity of polymer electrolytes including synthesizing various types of polymers with different architectures to achieve lowest possible T_g and suppression of crystallization of polymer chains to improve chain mobility.[7–9] Several researchers have reported the addition of carbonate-based plasticizers as chain lubricants to enhance the ionic conductivity by effectively decreasing the crystallinity of polymer electrolytes.[10,11] Though the magnitude of ambient conductivity is significantly enhanced using these carbonate-based organic liquids, these are highly flammable with low flash points and lead to safety hazards.[12,13]

In recent years, room temperature ionic liquids (RTILs) have been considered for electrolyte applications.[14–16] They are molten salts composed entirely of ions with low melting points and exist in liquid state at room temperature. Unlike liquid electrolytes, their unique properties such as negligible vapor pressure, high thermal and chemical stability, nonflammability, high ionic conductivity and wide electrochemical window makes them serious contenders as electrolytes in electrochemical processes and devices.[17–21] However, the issues of handling and leakage

Additional Supporting Information may be found in the online version of this article.

problems in ionic liquids (ILs) due to lack of structural integrity puts limitations in harnessing their outstanding electrochemical properties for device applications. This shortcoming is overcome by gelling ILs[22,23] using different approaches such as: (1) solidification of ILs by polymers[24–30]; (2) addition of inorganic nanoparticles,[31,32] carbon nanotubes,[33–35] and low-molar mass compounds,[36,37] and (3) Aqueous gelation of ILs.[38,39]

Specifically, ion-gels consisting of a swollen polymeric network in an IL constitute a promising class of solid state electrolytes owing to their combined advantages of good mechanical properties and high ionic conductivity which have potential applications in Li-ion batteries, electrochemical devices, sensors, electromechanical actuators, gas separation membranes, and dye-sensitized solar cells.[31,32,40–46] Most of the studies on ion-gels derived from polymers are based on doping of ILs with polymers and *in situ* polymerization (or crosslinking) of vinyl monomers in ILs.[22] For example, Watanabe and coworkers have synthesized transparent ion-gels with high ionic conductivity (~10 mS/cm) by *in situ* polymerization of methyl methacrylate (MMA) monomers in an imidazolium-based IL.[7] Carlin and coworkers have demonstrated the formation of stable gel electrolytes by doping poly(vinylidene fluoride)-hexafluoropropylene copolymer with 1-ethyl–3-methylimidazolium salts of triflate and tetrafluoroborate.[27] Recently, Lodge and coworkers have demonstrated the gelation of IL through the process of self-assembly of ABA triblock copolymer in a B-block compatible IL.[24,25] This is an attractive method of making solid electrolytes, which requires small amount of block copolymer to form ion-gels of sufficient mechanical strength and higher ionic conductivities. Unlike other methods such as chemical crosslinking to make ion-gels, this method affords thermally reversible sol–gel transition which offers liquid-state processing (similar to thermoplastics) and usage in solid-state and has opened unprecedented possibilities in the design of advanced materials for solid-state electrolyte applications.

Despite the availability of hundreds of ILs,[19] to our knowledge there are only three reports on ion-gels preparation based on gelation of two ILs ([BMIM][PF_6][24] and 1-ethyl-3-methylimidazolium bis(trifluoromethyl-sulfonyl)imide, [EMI][TFSI][25]), obtained from the self-assembly of block copolymers. It should also be noted that there is only one report in which the effect of concentration, temperature, and polymer identity on the ionic and viscoelastic motions of ion-gels is studied using Polystyrene (PS)-PEO-PS and PS-Poly(methyl methacrylate) (PMMA)-PS triblock copolymer in [EMI][TFSI], to design high performance electrolyte materials.[47] To expand the repertoire of functional polymer and IL composites and gels, systematic and comprehensive mechanical and electrical property evaluation of ion-gels formed via self-assembly of block copolymers is desirable. One of the objectives of this article is to demonstrate the gelation of IL, 1-butyl–3-methylimidazolium tetrafluoroborate ([BMIM][BF_4]) using poly (*N-tert*-butylacrylamide-*b*-ethylene oxide-*b*-*N-tert*-butylacrylamide) ($NtBAM_yEO_xNtBAM_y$, where x and y are number of repeat units) triblock copolymer through the process of self-assembly. The gelation arises from the noncovalent association of IL solvophobic *N-tert*-butylacrylamide terminal block, bridged by IL solvophilic EO mid block.

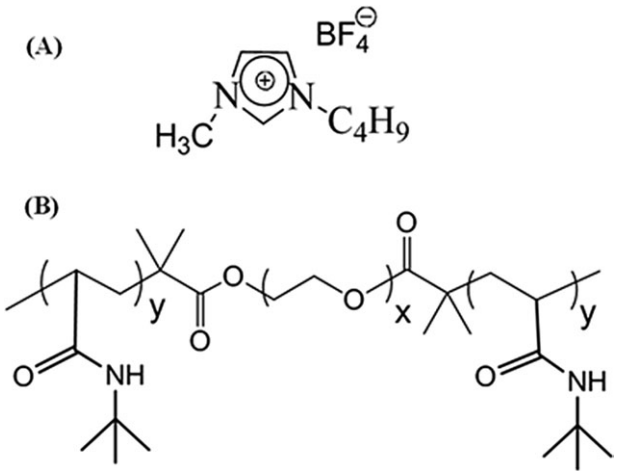

Figure 1. Chemical structures of 1-butyl-3-methylimidazolium tetrafluoroborate, [BMIM][BF_4] (A) and $NtBAM_yEO_xNtBAM_y$ triblock copolymer (B).

[BMIM][BF_4] has one of the highest conductivities observed in the general class of ILs and based on task-specific properties, it stands out as a good electrolyte solvent for lithium ion batteries due to its high ionic conductivity, Li-salt solubility at room temperature, and broad electrochemical window with high anodic stability (5 V) compared to other IL.[48–50] [BMIM][BF_4] ion-gels have been prepared previously by *in situ* copolymerization of acrylonitrile (AN), MMA, and poly(ethylene glycol) methyl ether methacrylate (PEGMEMA) in [BMIM][BF_4].[51] However, these ion-gels are formed at high copolymer concentration (> 30 wt %) which significantly lowers their ionic conductivity as compared to the bulk [BMIM][BF_4] and limits their applications. Nevertheless, there have been neither reports on the gelation of [BMIM][BF_4] by macromolecular self-assembly nor mechanical, thermal, and conductivity investigations of the corresponding ion-gels. Thus, the current study focuses on designing highly conductive, mechanically robust ion-gels of [BMIM][BF_4] at low copolymer concentration so that conductivity of these ion-gels is comparable to the bulk IL. To the best of our knowledge, this is the first effort to gel [BMIM][BF_4] by macromolecular self-assembly of block copolymers and comprehensive structure–property and conductivity investigations of the corresponding ion-gels.

EXPERIMENTAL

Materials

N-tert-butylacrylamide (Acros organics, Pittsburgh, PA), 1, 4-dioxane (Aldrich, St. Louis, MO, 98%), [BMIM][BF_4] (Aldrich), and 2,2′-Azobisisobutyronitrile (AIBN, Aldrich, 98%) are used as received. PEO is purchased from Aldrich (M_v = 35,000 g/mol, $M_{n,GPC}$ = 26,000 g/mol). A RAFT (reversible addition-fragmentation chain transfer) based chain transfer agent (CTA), dodecyl-S′-(α,α′-dimethyl-α″-aceticacid) trithiocarbonate is prepared according to a published work by Lai et al.[52] [BMIM][BF_4] is a colorless room temperature hygroscopic IL with a density of 1.20 g/cm^3 and viscosity of 75 mPa s at 25°C.[50,53] The ionic conductivity (σ) of the bulk [BMIM][BF_4] is 3.5 mS/cm at 25°C.[50] The chemical structure of the IL is shown in Figure 1(A).

Polymerization

Synthesis of Macromolecular Chain Transfer Agent, CTA-EO_{592}-CTA. The macromolecular CTA, CTA-EO_{592}-CTA, is prepared according to a reported procedure.[25] CTA (0.26 g, 0.71 mmol) is dissolved in 25 mL dichloromethane in an air-free flask capped with rubber septa and connected to a bubbler. The flask is purged with N_2 for 20 min, after which oxalyl chloride (0.30 mL, 3.55 mmol) is injected into the flask for 15 min. The mixture is stirred under N_2 atmosphere for about 2 h until the gas evolution stops. The volatiles are then removed under vacuum. The flask is again purged with N_2, and then 40 mL dichloromethane solution of PEO 26,000 g/mol (5 g, 0.19 mmol, 0.38 mmol OH endgroups) is added through a cannula. The reaction is allowed to proceed for 24 h. The product is precipitated in *n*-hexane and washed numerous times with *n*-hexane to remove unreacted CTA and dried *in vacuo* at room temperature (Light yellow powder, yield 95%). ^{1}H-NMR ($CDCl_3$, δ ppm): 4.25 (t, 2H, —COOCH_2— in EO end group), 3.62 (m, —CH_2CH_2O—, repeating units of EO), 3.25 (t, 2H, $CH_3C_{10}H_{20}CH_2$—S—), 1.50–1.75 (m, 6H, —S—C(CH_3)$_2$COO—), 1.25 (m, 20H, $CH_3C_{10}H_{20}CH_2$ S—), 0.87 (t, 3H, C$H_3C_{10}H_{20}CH_2$ S—).

Synthesis of Triblock Copolymer Using Ethylene Oxide Macro Chain Transfer Agent (CTA-EO_{592}-CTA). A series of triblock copolymers are prepared and their chemical structure is shown in Figure 1(B). The representative procedure of synthesizing sample $NtBAM_{24}EO_{592}NtBAM_{24}$ is described here. CTA-EO_{592}-CTA (3 g, 0.0857 mmol), *N-tert*-butylacrylamide (2.74 g, 21.5 mmol), and AIBN (106.25 mg, 0.647 mmol) are dissolved in 1,4-dioxane (100 mL) in an air-free flask equipped with a stir bar. The flask is then sealed with a rubber septum and degassed by purging N_2 for 30 min. After that the flask is placed in a 75°C oil bath and the reaction is allowed to proceed for 24 h. The contents are precipitated in excess of *n*-hexane, filtered, and dried in vacuum oven for 24 h. The chemical structure of the triblock copolymer is shown in Figure 1(B). ^{1}H-NMR ($CDCl_3$, δ ppm): 1.0–2.3 (br, CH_3, CH_2, C*H*), 3.4–3.9 (br, CH_2) and 5.5 (br, N*H*) ppm. Gel permeation chromatography (GPC) (40°C, Tetrahydrofuran (THF) mobile phase, polystyrene standards): $M_{n,\mathrm{NtBAM}} = 6000$ g/mol, polydispersity indices (PDI) = 1.22.

Characterization

^{1}H-NMR (500 MHz) spectra is recorded on a Bruker DMX-500 at 24°C in $CDCl_3$ (Aldrich; 0.03% vol/vol TMS as an internal standard). The number-average molecular weight (M_n) and weight percentage of *N-tert*-butylacrylamide (NtBAM) in the triblock copolymer is determined by ^{1}H-NMR spectroscopy. GPC analysis is performed at 40°C on a Waters 150-C Plus gel permeation chromatograph equipped with a Waters 2487 dual wavelength absorbance UV–vis detector set at 254 nm, a Polymer laboratories PL-ELS 1000 evaporative light scattering detector, and with a Jordi Flash Gel 105 Å, 2 × 104 Å, 1 × 103 Å column setup. THF (Fisher; 99.9% High-performance liquid chromatography (HPLC) grade) is used as an eluent at a flow rate of 2 mL/min. The PDI are determined using calibration plots from polystyrene standards.

Preparation of Sol and Gels

The triblock copolymers in the present study have significant weight fraction of *N-tert*-butylacrylamide block and therefore it was difficult to prepare solutions and gels by direct dissolution of triblock copolymers in [BMIM][BF_4]. To prepare stable solutions and gels, we followed co-solvent aided dissolution method. In this procedure, a pre-weighed triblock copolymer is first dissolved in dichloromethane (DCM), a common solvent for both the blocks, with subsequent addition of [BMIM][BF_4] to get the desired concentration. The sample is set aside in a hood for 2 weeks at ambient temperature and DCM was removed by gradual evaporation. Thereafter, the mixture is maintained at (80 ± 5)°C for 6 h and optically clear solutions and gels are obtained. In this study, the concentration is expressed in wt %. The prepared solutions and ion-gels are stored in air-tight vials and aged for a week at room temperature prior to rheological experiments. Newly prepared samples are used for each experiment.

Rheology. The rheological properties of triblock copolymer solutions and ion-gels are analyzed using the AR-G2 rheometer (TA Instruments, minimum torque oscillation: 0.003 μN m and torque resolution: 0.1 μN m) with peltier plate-temperature control. A cone-plate geometry with a diameter, $d = 40.0$ mm, and cone angle (deg : min : s = 1 : 59 : 24), is used for more fluid-like samples with approximately 2 mL of sample added at experimental temperatures. Parallel plate geometry (20 mm diameter) is used for more solid-like samples. Dynamic frequency sweep experiments are performed from 10^{-2} to 10^2 rad/s between 10 and 100°C while cooling the samples. Dynamic temperature ramp experiments are performed to determine the temperature dependent rheological properties by heating the samples at a rate of 1°C/min and oscillation frequency (ω) 0.1 rad/s. Only linear viscoelastic properties are measured for dynamic frequency and temperature ramp experiments and the linear range is determined using strain sweep experiments. Strength of the ion-gels is qualitatively ascertained by running dynamic strain sweeps at oscillation frequency (ω) of 6.283 rad/s. In each experiment, 30 min conditioning time is allowed for thermal equilibration and to get rid of any shear history introduced while transferring the copolymer solutions to the appropriate geometry.

Thermogravimetric Analysis. Thermogravimetric analysis (TGA) measurements were performed on the ion-gels using a Hi-Res TGA-2950 thermogravimetric analyzer (TA instruments) from 20°C to 800°C at a heating rate of 20°C/min in air.

Ionic Conductivity Measurements. The ionic conductivity (σ) measurements are carried out in an in-house designed and machined cell using an Agilent 4284A Precision LCR meter. The amplitude of the AC voltage signal is 10 mV and the applied frequency range is 20 Hz to 60,000 Hz. The solutions and gels are heated at 90–100°C and then filled into the multi-sample cell consisting of two stainless steel blocking electrodes separated by a teflon ring of diameter ($d = 22.2$ mm) and thickness ($L = 2.05$ mm). The cell is calibrated using a 0.1*N* aqueous KCl standard solution at 25°C. Before each conductivity measurement, the sample cell is equilibrated at the testing temperature for 20–30 min. Since [BMIM][BF_4] is hygroscopic, all measurements are performed under stringent experimental conditions to prevent any significant moisture absorption from air and

repeated for reliability of data. The reported conductivity values for bulk [BMIM][BF_4], solutions, and ion-gels are based on the measurements from three repetitions in the temperature dependent experiments. Error bars in the plots are reported as standard error of the averaged values of conductivity (σ).

RESULTS AND DISCUSSION

As stated previously, [BMIM][BF_4] has one of the highest conductivities observed in the general class of ILs and has been used as an electrolyte solvent for lithium ion batteries due to its high ionic conductivity, Li-salt solubility at room temperature, and broad electrochemical window with high anodic stability (5 V) compared to other ILs. We are interested in obtaining ion-gels of [BMIM][BF_4] with tunable mechanical and electrical properties using macromolecular self-assembly of block copolymers at low concentrations in this IL as a better alternative to chemical gelation using high concentration of polymers. General perusal of literature shows that [BMIM][BF_4] may be gelled using block copolymers with PEO as the IL soluble block.[54,55] Solubility experiments performed in our laboratory suggests that poly(*N-tert*-butylacrylamide) homopolymer remains insoluble in [BMIM][BF_4] over a temperature range of 25–100°C and therefore suggests *N-tert*-butylacrylamide moiety can be used as an IL-solvophobic block in block copolymers. We have previously reported the synthesis of *N-tert*-butylacrylamide-based block copolymers[56,57] and have used a similar controlled-radical based synthetic strategy to prepare triblock copolymers with EO as the central block and *N-tert*-butylacrylamide as the end blocks. These block copolymers were further used to gel [BMIM][BF_4]. The use of glassy *N-tert*-butylacrylamide block (T_g = 128°C)[58] allows the formation of junctions in the gel network due to its insolubility in [BMIM][BF_4], which predominantly provides mechanical robustness to the corresponding ion-gels. Thus, the synthesis of these block copolymers provides us a handle to explicitly tune the mechanical properties of the ion-gels.

Synthesis and Molecular Characterization of Macrochain Transfer Agent and Triblock Copolymer

Detailed synthetic protocol to prepare triblock copolymers are discussed in the experimental section. In the first step, macromolecular chain transfer agent CTA-EO_{592}-CTA is prepared through the coupling reaction between the hydroxyl end groups of EO and the CTA acid chloride (Supporting Information Figure S1).[25] To ensure that both ends of the EO have been modified by CTA, a large excess of CTA with respect to EO is used ([CTA] : [EO] = 3.7 : 1). In the second and final step, using CTA-EO_{592}-CTA as the macromolecular CTA, *N-tert*-butylacrylamide as monomer, and AIBN as radical initiator, triblock copolymers ($NtBAM_yEO_xNtBAM_y$) are prepared (Supporting Information Figure S1) and the results of polymerization are summarized in Table I.

The molecular weights and composition of the triblock copolymers are summarized in Table I. All the GPC traces of the triblock copolymers are unimodal (Supporting Information Figure S2). In the ^{1}H-NMR spectra of a representative sample, $NtBAM_{24}EO_{592}NtBAM_{24}$ (Supporting Information Figure S3), protons of *N-tert*-butylacrylamide end block appears at a, c, d, and e corresponding to —NH—, —CH—, —CH_2—, and —CH_3— (*tert*-butyl) protons of the substituent group, respectively, in addition to the —CH_2— signals of EO block.[59,60] ^{1}H-NMR is used to determine the number-average molecular weight (M_n) and copolymer composition in $NtBAM_yEO_{592}NtBAM_y$.

Table I. Molecular Characteristics of Poly(*N*-tert-butylacrylamide-*b*-ethyleneoxide-*b*-*N*-*tert*-butylacrylamide), $NtBAM_yEO_{592}NtBAM_y$

Entries	Polymer	Wt % (NtBAM block) (NMR)	$M_{n,NtBAM}$[a] (g mol^{-1}) (NMR)	M_w/M_n (GPC)
1	$NtBAM_{24}$ $EO_{592}NtBAM_{24}$	19	6,000	1.22
2	$NtBAM_{41}$ $EO_{592}NtBAM_{41}$	29	10,500	1.24
3	$NtBAM_{51}$ $EO_{592}NtBAM_{51}$	33	13,000	1.33

EO: ethylene oxide block; NtBAM: *N-tert*-butylacrylamide block.
[a]Total M_n of the acrylamide block in the triblock copolymer; molecular weight (M_n) of PEO homopolymer from GPC: 26,000 g mol^{-1}. The subscripts in $NtBAM_yEO_{592}NtBAM_y$ are number of repeat units.

Gelation of [BMIM][BF_4] Using $NtBAM_yEO_xNtBAM_y$ Triblock Copolymer: Strong Ion-Gels

Using triblock copolymers of different NtBAM block length, stable solutions and ion-gels are formed in [BMIM][BF_4]. Sol–gel transition can easily be determined by tube inversion tests and rheology. Sol–gel transitions and preliminary phase diagram of the copolymer solutions at room temperature is mapped by tube inversion experiments in which the sample

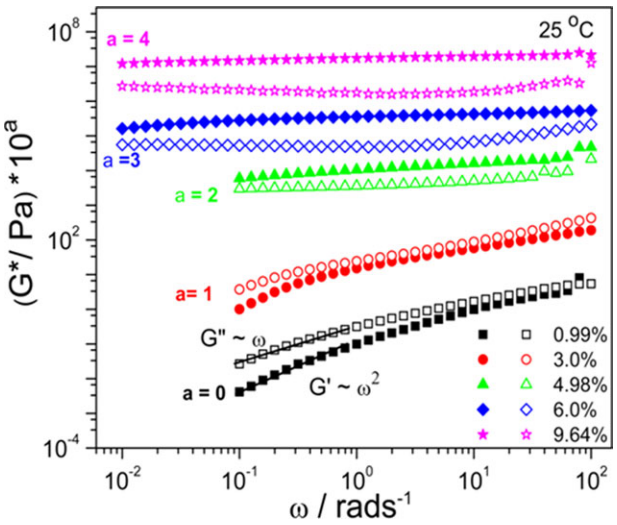

Figure 2. Storage modulus (G') and loss modulus (G'') (filled and open symbols) versus angular frequency (ω) of $NtBAM_{51}EO_{592}NtBAM_{51}$ in [BMIM][BF_4] for various concentrations at 25°C. The curves at different concentrations are shifted vertically by the factor 10 ^{a} as indicated to avoid overlapping. [Color figure can be viewed in the online issue, which is available at wileyonlinelibrary.com.]

Applied Polymer SCIENCE

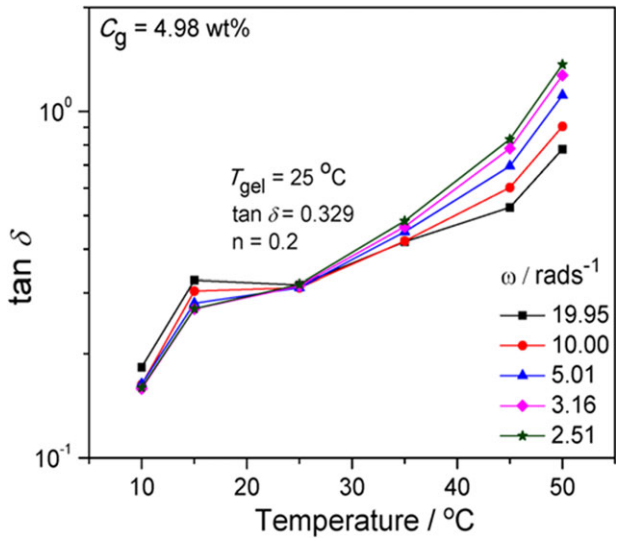

Figure 3. Loss tangent, tan δ as a function of temperature for NtBA-$M_{51}EO_{592}NtBAM_{51}$/[BMIM][BF_4] system at various angular frequencies with C_g = 4.98 wt %.[Color figure can be viewed in the online issue, which is available at wileyonlinelibrary.com.]

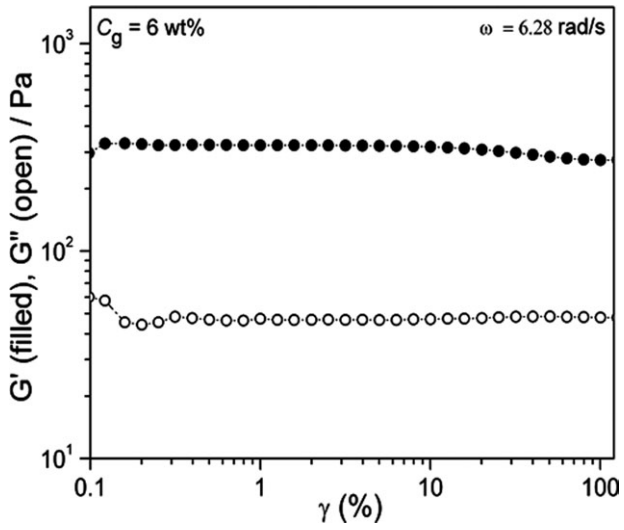

Figure 4. Strain dependence of complex modulus (G^*) for NtBA-$M_{51}EO_{592}NtBAM_{51}$/[BMIM][BF_4] system with C_g = 6 wt % at 25°C.

having a yield stress (gel or elastic solid) will not flow whereas a viscous but inelastic sample (sol) will show an appreciable flow when tube containing sample is inverted, as shown in Table II. Interestingly, the sol–gel transition for triblock copolymers with 24, 41, and 51 repeat units of NtBAM (on each end of the copolymer) occurs at 12, 8, and ~5 wt %, respectively. This data is indicative of the general trend of critical gelation concentration for these polymers to form gels in IL, which decreases with increasing NtBAM block length.

Sol–gel transitions and mechanical properties of these ion-gels are comprehensively investigated using rheology. In Figure 2, frequency dependence of real (G') and imaginary (G'') part of the complex modulus (G^*) is plotted over a concentration range for $NtBAM_yEO_{592}NtBAM_y$/[BMIM][BF_4] at 25°C. Lower concentrations (1 wt %) of these triblock copolymer solutions behaves as viscoelastic fluids in the terminal frequency range with storage modulus (G') smaller than the loss modulus (G'') and are described by the scaling relationship: $G'(\omega) \sim\omega^2$, $G''(\omega) \sim\omega^1$ (at $\omega \rightarrow 0$).[57,61] Both $G'(\omega)$ and $G''(\omega)$ increases with concentration of the copolymer in [BMIM][BF_4], and eventually an optically transparent gel is obtained above a critical gelation concentration, $C_g \geq$ 5 wt %. Above C_g, $G'(\omega) > G''(\omega)$ and is nearly frequency independent in the terminal frequency range which is a characteristic of solid-like behavior. The gel-like behavior indicated by the evolution of quasi-equilibrium modulus manifests as a gel plateau following a scaling relationship: $G'(\omega) = G_e$ (at $\omega \rightarrow 0$).[57,61] Additional data for sol–gel transitions of $NtBAM_{24}EO_{592}NtBAM_{24}$ and NtBA-$M_{41}EO_{592}NtBAM_{41}$ in [BMIM][BF_4] are shown in Supporting Information Figure S4.

Winter and Chambon gelation criterion[62,63] is used to determine the gelation temperatures (T_{gel}) of these ion-gels. According to this criterion, gel point is exhibited by a power-law behavior as shown in eqs. (1) and (2) such that gelation variable loses its dependency on the frequency and converges at a point which is critical gelation temperature (T_{gel}) in this case. Frequency independence of loss tangent (tan δ) in the vicinity of gel point has been widely used for physical and chemical gels to determine the critical gelation variable.[62,64,65]

$$G' \sim (\omega)G''(\omega)\omega^n (0 < n < 1) \quad (1)$$

Or

$$G''(\omega)/G'(\omega) = \tan\delta = \tan(n\pi/2) \quad (2)$$

where n is defined as a viscoelastic exponent whose value lies between 0 and 1. Applying this criterion, Figure 3 shows a multi-frequency plot of tan δ versus temperature for 5 wt % of

Table II. Tube Inversion Test of $NtBAM_yEO_{592}NtBAM_y$/[BMIM][BF_4] Triblock Copolymer Solutions

conc. (wt %)	6	7.61	10	12	14.80	20
$NtBAM_{24}EO_{592}NtBAM_{24}$	m	m	m	m+g	g	g
conc. (wt %)	6	8	10	11.90	14.90	21
$NtBAM_{41}EO_{592}NtBAM_{41}$	m	m+g	g	g	g	g
conc. (wt %)	3	4.94	6	8	10	12
$NtBAM_{51}EO_{592}NtBAM_{51}$	m	m+g	g	g	g	g

m: micellar solution or sol; m + g: mixture of micelle and gel near the gelation point; g: gel.

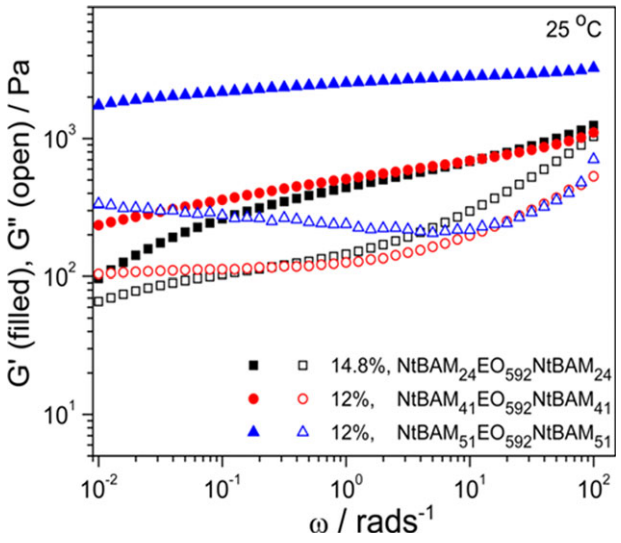

Figure 5. Storage modulus (G') and loss modulus (G'') versus angular frequency (ω) for ion-gels with increasing NtBAM block length for series of copolymers: $NtBAM_{24}EO_{592}NtBAM_{24}$, $NtBAM_{41}EO_{592}NtBAM_{41}$, and $NtBAM_{51}EO_{592}NtBAM_{51}$ at concentrations of 14.8, 12, and 12 wt % respectively. [Color figure can be viewed in the online issue, which is available at wileyonlinelibrary.com.]

$NtBAM_{51}EO_{592}NtBAM_{51}$/[BMIM][$BF_4$] system, in which the curves passes through a common point known as T_{gel}, determined to be 25°C. Thus at 25°C, 5 wt % exhibits a power-law: $G'(\omega) \sim G''(\omega) \sim \omega^{0.2}$ which is a signature of the transition between liquid-like and solid-like behavior at gel point. In a similar manner, we obtained critical gelation temperature for 6 wt % ion-gels, $T_{gel} = 45$°C much higher than room temperature as shown in Supporting Information Figure S5. Thus, unlike previous studies in which [BMIM][BF_4] ion-gels were formed at >30 wt %,[51] we demonstrate the formation of ion-gels at room temperature for as low as 5 wt % copolymer mass in a predominantly conducting phase of IL.

In all the polymers discussed here, the EO block length is constant and the effect of NtBAM block length on the C_g is investigated. In this library of triblocks, the lowest C_g value of ~5 wt % is seen in the case of $NtBAM_{51}EO_{592}NtBAM_{51}$, while highest C_g of ~15 wt % is observed for $NtBAM_{24}EO_{592}NtBAM_{24}$. Interestingly, a two-fold increase in the molecular weight of IL-solvophobic NtBAM block lowers the C_g by three-folds. From the literature, it is also widely known that temperature and concentration range where gels are formed can be tuned by varying solvophilic and solvophobic blocks. Studies on PEG-poly(lactic acid-*co*-glycolic acid) (PLGA)-PEG hydrogels[66] have shown sol–gel transition to be sensitive toward the hydrophobic PLGA block and gelation is shifted toward lower concentrations with increasing PLGA block length. It is well-established that physically associating triblock copolymers in mid block selective solvent results in aggregates due to insolubility of the solvophobic end blocks. Above a critical concentration, a certain fraction of the mid block will form bridges between the end block domains, resulting in the formation of an elastic network or gel.[67,68] In our system, with increase in block length (or molecular weight) of the solvophobic end block, the tendency to bridge becomes much more easier and dominant at lower concentrations resulting in elastic gels. Thus these observations reflect the impact of acrylamide block length on gelation behavior of this triblock copolymer-IL system.

We are interested in exploring the ability of these ion-gels to withstand large deformations which is important with regards to their applications. Strong ion-gels are desirable in most of the device application as there should be no fracture or failure during processing and usage of these gelled electrolytes which otherwise affects their performance. We observed that vigorous stirring of the ion-gel breaks the structure and it recovers only on melting and subsequent resetting. To confirm that we were able to make strong gels, we performed large deformation experiments proposed by Rossmurphy and Shatwell.[69] The complex modulus (G^*) for strong gels is mainly strain independent (linearly viscoelastic) for strains up to 25% and for weak gels G^* becomes strain dependent when strain is greater than 5%.[70] In Figure 4, oscillatory shear strain sweep measurements have shown that G' remains strain invariant up to very high values of strain (>> 25%) indicating the formation of strong ion-gels, which can withstand mechanical stress required for device applications. Large deformation experiments of other ion-gel compositions are shown in Supporting Information Figure S6.

Effect of NtBAM Block Length on the Elastic Modulus (G_e) of Ion-Gels and Scaling of G_e with Copolymer Concentration

Figure 5 compares the elastic modulus of the copolymer series with 24, 41, and 51 NtBAM repeat units at concentrations of 14.8, 12, and 12 wt %, respectively, at 25°C. Although the gel obtained from copolymer with 24 repeating units of NtBAM is compared at 14.8 wt %, as opposed to 12 wt % of other copolymer gel samples, it still forms a weaker gel. As the length of the solvophobic acrylamide block is increased from 24 to 51, gel strength improves by an order of magnitude from ~100 Pa to >1000 Pa. For further comparison, it is also worth mentioning that G' of a 6 wt % ion-

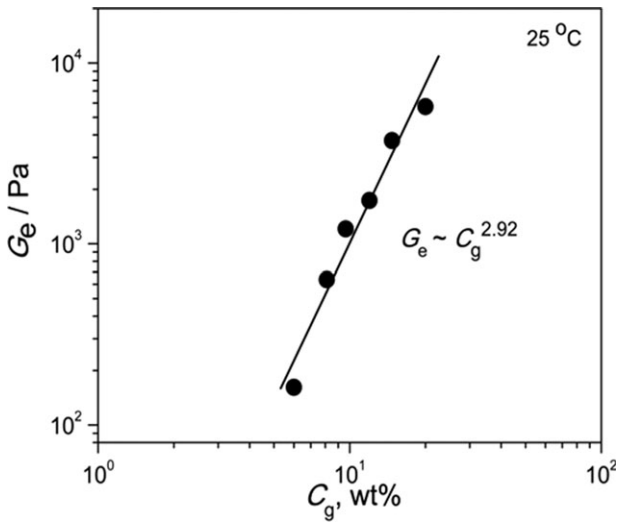

Figure 6. Gel modulus G_e of the ion-gels versus copolymer concentration on a double logarithmic scale for $NtBAM_{51}EO_{592}NtBAM_{51}$/[BMIM][$BF_4$] system at 25°C.

Applied Polymer SCIENCE

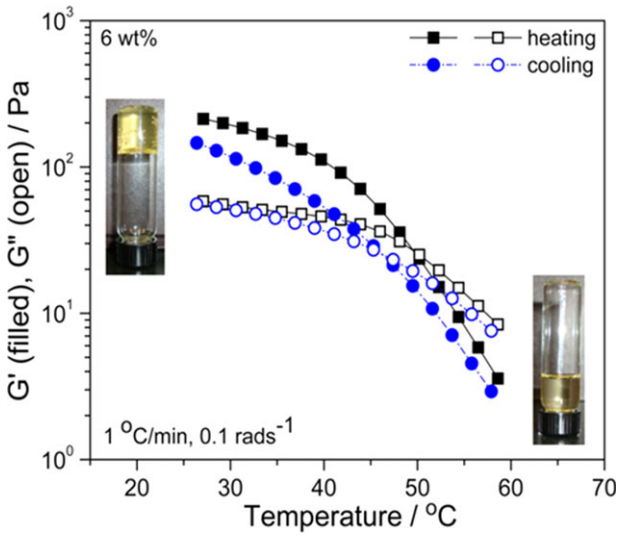

Figure 7. Storage modulus G' and loss modulus G'' of $NtBAM_{51}EO_{592}NtBAM_{51}$/[BMIM][$BF_4$] ion-gel as a function of temperature at an angular frequency ω of 0.1 rad/s with indicated concentration, C_g = 6 wt %. [Color figure can be viewed in the online issue, which is available at wileyonlinelibrary.com.]

gel derived from copolymer with 51 NtBAM repeat units has similar modulus (~100 Pa) to the copolymer with 24 NtBAM repeat units at 14.8 wt %. Similar trends have been observed in PLLA-PEO-PLLA hydrogels[71] in which G' shows strong dependence on the PLLA end block length of a triblock copolymer. Thus, the dependence of the elastic modulus (G') on the acrylamide (NtBAM) length offers a straightforward way to tune the rheological response of these ion-gels.

The quasi-equilibrium modulus (G_e) is a measure of density of elastically active crosslinks or long-lived junctions in a network structure formed as a result of intermolecular aggregation. The effect of concentration on the equilibrium modulus (G_e) in $NtBAM_{51}EO_{592}NtBAM_{51}$/[BMIM][$BF_4$] system is shown in Figure 6. A noteworthy feature is that with increase in copolymer concentration, the elastic modulus (G_e) also increases, implying that the number of long-lived junctions in the gel increases. Interestingly, G_e increases linearly with the cube of C_g on a double logarithmic scale and yields a scaling relation: $G_e \sim C_g^{2.92}$. In literature, different scaling behaviors are expected from entangled network of polymers, semi-dilute polymer solutions, and flexible chemical gels (exponent of 2.25)[72] and concentrated polymer solutions (exponent of 2).[73] For associative polymer networks and physical gels, a cubic relationship is found for the moduli, $G_e \sim C_g^{3.1}$,[74] and the result found in our ion-gels agrees well with this predicted scaling value (3.1). We can also relate the moduli of ion-gels to the shear modulus of a semi-dilute polymer network, $G_e \sim k_bT/\xi^3$, where k_b is the Boltzmann constant and ξ is the correlation length associated with the network mesh size.[72,75] Comparing the two scaling relationships, mesh size varies inversely with the copolymer concentration, $\xi \sim 1/C_g$, i.e. mesh size of the network decreases as we add more and more copolymer above critical gel concentration. It is important to note that the tunability of the mesh size in a gel network affects the diffusion of the ionic species which ultimately impacts the ionic conductivity of these ion-gels.

Thermoreversibility and Thermal Stability Studies

Thermoreversibility and thermal stability are important parameters for liquid state processing and material usage at different temperatures, respectively. Heating–cooling cycles of the ion-gels in the dynamic temperature ramp measurements confirmed their thermoreversible behavior as shown in Figure 7 (additional plots shown in Supporting Information Figures S7 and S11). Indeed, the cross-over of G' and G'' occurs at 46°C in the cooling cycle, a lower temperature than that determined in the heating cycle (50°C). The difference in the cross-over temperature between the heating and cooling cycles is due to the kinetics between the association and dissociation processes.[76,77] Gel-fluid phase transition (see Figure 8), shows G' and G'' as a function of temperature at frequency of 0.1 rad/s for ion-gel samples. The copolymer concentration was varied from 5 to 20 wt %. All the samples are in a gel state at room temperature; G' decreases with increasing temperature and at a given temperature the cross-over of G' and G'' gives the melting temperature (T_c) of the ion-gels. Furthermore, the melting temperature (T_c) can be easily tuned over a wide temperature range by varying the copolymer concentration, which is important for tuning the processing parameters and application temperatures of these gels. The ion-gels are subjected to various heating and cooling cycles during experiments and there are always chances of thermal degradation which adversely affects its mechanical properties and potential applications. Thermogravimetric measurements (TGA) performed on these ion-gels in air show a weight loss of 1–4% at 200°C (see Figure 9), confirming their high thermal stability. In contrast, the [BMIM][BF_4] gels prepared by Qi and coworkers[51] are stable up to 120°C in N_2 atmosphere.

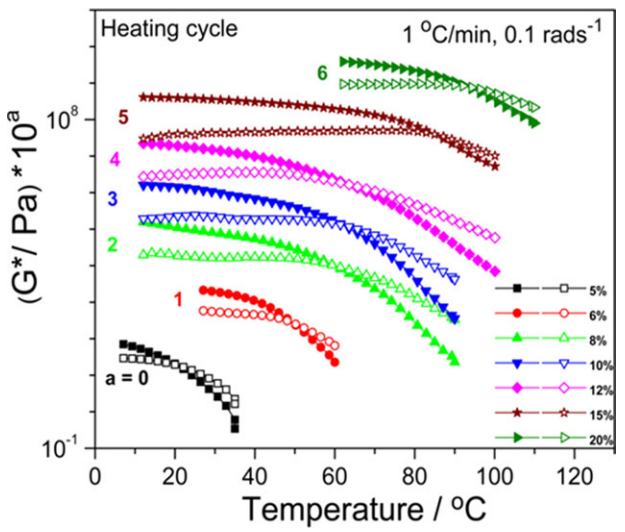

Figure 8. Temperature dependence of the storage modulus G' (filled) and loss modulus G'' (open) for $NtBAM_{51}EO_{592}NtBAM_{51}$/[BMIM][$BF_4$] ion-gels with indicated concentration, (C_g: 5, 6, 8, 10, 12, 15, 20 wt %). The curves at different concentrations are shifted vertically by the factor 10^a as indicated to avoid overlapping. [Color figure can be viewed in the online issue, which is available at wileyonlinelibrary.com.]

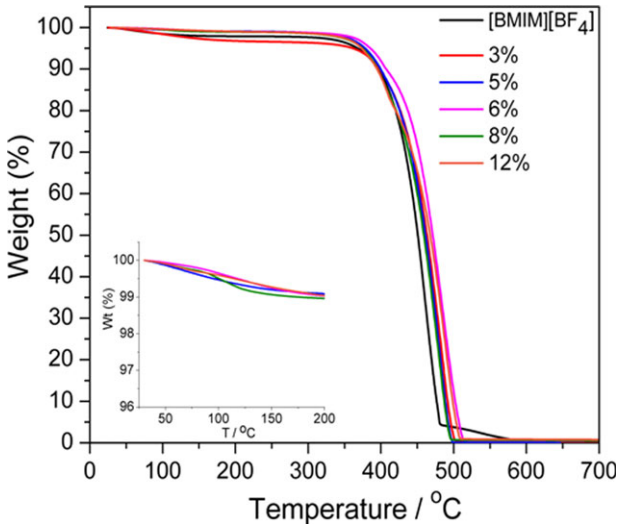

Figure 9. Weight percentage change (%) versus temperature for bulk [BMIM][BF_4] and $NtBAM_{51}EO_{592}NtBAM_{51}$/[BMIM][$BF_4$] solutions and ion-gels. [Color figure can be viewed in the online issue, which is available at wileyonlinelibrary.com.]

Weight loss at 100°C provides information of the relative amount of water present in pure IL and triblock copolymer solutions. From the TGA measurements shown in Figure 9, there is around 1% and 0.5% weight loss at 100°C for pure IL and triblock copolymer/IL solutions (and gels) respectively which suggests an insignificant amount of water in these systems.

Ionic Conductivity

The conductivity of the solutions and ion-gels is calculated from the measured complex impedance ($Z^* = Z' - iZ''$). The impedance data is represented in a Bode plot, in which the magnitude of the complex impedance ($|Z^*|$) and phase angle (θ) is plotted as a function of frequency (f). Supporting Information Figure S8 shows a typical Bode plot of $|Z^*| - f$ and $\theta - f$ for $NtBAM_{51}EO_{592}NtBAM_{51}$ with $C_g = 6$ wt % at 23°C. At lower frequencies, polarization effects result in frequency-dependent impedance data ($|Z^*| \propto \omega^{-a}$, $0 < a < 2$), while at high frequencies the impedance spectra is dominated by ionic mobility, resulting in a frequency-independent $|Z^*|$ plateau. The phase angle (θ) shows a minimum at higher frequencies. Both the frequency-independent plateau in $|Z^*|$ and the minimum in phase angle (θ) depend on polymer concentration and experimental temperatures. The sample resistance R is read as the frequency-independent ($|Z^*|\cos\theta$) value in the Bode plot, i.e., $R = |Z^*|\cos\theta$ which is further used to calculate the ionic conductivity (σ) using the following formula[78]:

$$\sigma = \frac{1}{R}\left(\frac{L}{A}\right) \tag{3}$$

where L is the sample thickness and A is the contact area of electrodes.

Frequency and Temperature Dependent Conductivity Studies

We are interested in thoroughly understanding the conductivity (σ) of these ion-gels as a function of frequency and temperature which will be important for device applications. We have confined our studies to $NtBAM_{51}EO_{592}NtBAM_{51}$/[BMIM][$BF_4$] system which formed ion-gels at lowest concentration (~5 wt %). This allowed us to explore materials which have optimal mechanical integrity at low copolymer mass. Figure 10 shows a log–log plot of σ as a function of frequency (f) for bulk [BMIM][BF_4] and different gel concentrations (C_g). The logarithmic plots can be divided into two regions: (i) a low frequency dispersion region and (ii) a frequency-independent plateau region. The low frequency dispersion region may be due to the interfacial impedance or space charge polarization where more and more ionic species gets accumulated at the electrode and electrode-ion-gel interface due to the slow periodic reversal of the electric field, which will result in a decrease of carrier-ions and eventually a decrease in σ. On the contrary, in the high frequency regime, a relatively small number of ions can accumulate at the electrode and the interface, which results in higher number density of mobile ions (or charge carriers) and a plateau is formed, which is equivalent to the true dc conductivity—typical of polymer electrolytes.[10,79,80] The high frequency conductivity (see inset in Figure 10) of the ion-gels is in the range of (1–3) mS/cm at room temperature which is much higher than the maximum reported conductivity of solid polymer electrolytes (0.01–0.1 mS/cm).[81]

The temperature dependent conductivity of the bulk [BMIM][BF_4] and the ion-gels at different concentrations of 6, 8, 10, and 15 wt % is shown in Figure 11 in the Arrhenius convention (x-axis reversed). The σ of ion-gels increases with increase in temperature, which can be explained on the basis of the Walden's rule[82]: the product of conductivity (σ) and viscosity of the pure solvent is a constant for all temperatures and solvents for a given electrolyte, $\sigma\eta$ = constant. With increasing

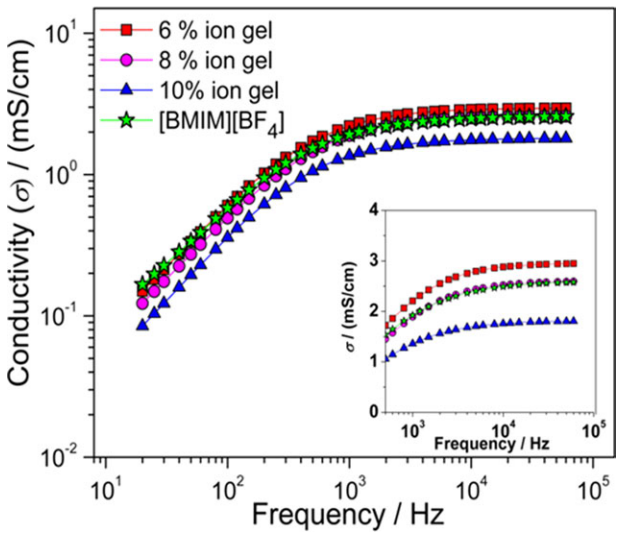

Figure 10. Frequency dependence of the ionic conductivity (σ) for bulk [BMIM][BF_4] and various concentrations of $NtBAM_{51}EO_{592}NtBAM_{51}$/[BMIM][$BF_4$] ion-gels at room temperature. Inset: Semi-log plot of σ as a function of frequency in the high frequency region ($f \geq 1$ kHz). [Color figure can be viewed in the online issue, which is available at wileyonlinelibrary.com.]

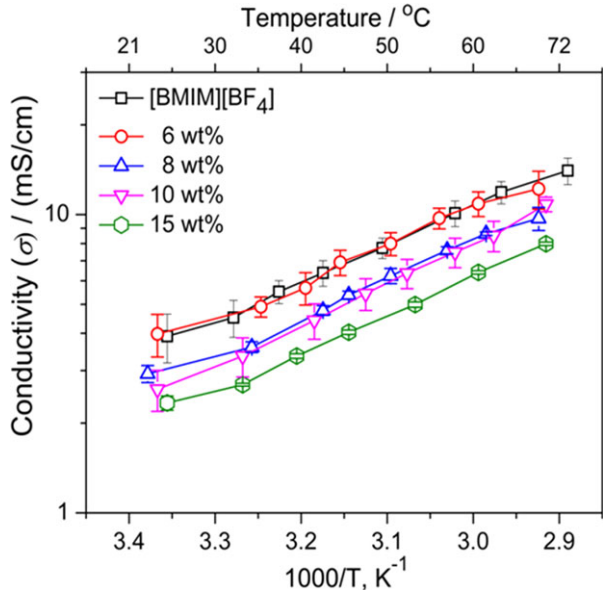

Figure 11. Ionic conductivity (σ) as a function of temperature for bulk [BMIM][BF_4] and ion-gels (6, 8, 10, and 15 wt %) for $NtBAM_{51}EO_{592}NtBAM_{51}$/[BMIM][$BF_4$] system. Error bars in the plot represent standard error of σ for three independent experiments. [Color figure can be viewed in the online issue, which is available at wileyonlinelibrary.com.]

temperature, the viscosity decreases, making ions more mobile resulting in an increased σ (also see Supporting Information Figure S9). The conductivity of 6 wt % ion-gel is similar to that of the bulk IL. Interestingly, as seen in Figure 11, the temperature dependence of σ for all concentrations of the ion-gel nearly tracks the σ of bulk IL. A similar observation of temperature dependent σ and proportionality of σ and $1/\eta$ is also seen in PS-PEO-PS/[BMIM][PF_6] based ion-gels.[24] In Figure 11, the temperature dependence of σ does not show any change in steepness with increasing copolymer concentrations in the low temperature range. This suggests that in our system, glass transition temperature of ion-conducting EO phase ($T_{g,\ PEO}$) does not affect the mobility of the ionic species and hence σ, which is very different from the trend reported by Segalman and coworker.[83] The pronounced effect of glass transition temperature on σ is clearly demonstrated in a recent work by Segalman and coworker, where temperature dependence of σ in P2VP/[IM][TFSI] becomes less steep with decreasing copolymer mass (or increasing mass of IL) and is correlated with the decrease of glass transition temperature (T_g) of ion conducting P2VP phase.[83]

Effect of Concentration on the Ionic Conductivity (σ)

Figure 12 shows the concentration dependence of σ for $NtBAM_{51}EO_{592}NtBAM51$/[BMIM][$BF_4$] system at room temperature. σ of the ion-gels decreases with increase in copolymer concentration compared to the bulk IL. The influence of concentration on σ can be described as contributions from two processes: (i) diffusion of ions in the polymer network and (ii) polymer–IL interactions. The presence of a polymer network in IL has a physical blocking effect on the diffusion of ions resulting in a restricted diffusion and eventually decreased conductivity.[84] Additionally, the chemical interactions between the polymer and IL may also affect the carrier ion concentration. ILs appears as free ions and ion aggregates or clusters[85,86] and the latter are neutral species that do not participate in the conduction mechanism. The interaction of polymer with IL decreases the possibility of cluster formation by dissociating the latter resulting in an increase in the number of charge carriers and hence the σ becomes higher than the bulk IL.[7] At copolymer concentration, $C_g \geq 6$ wt %, the system exist in a gel state and the two competing factors influence the final σ. Obstruction effects on the σ of ion-gels are substantiated by qualitatively comparing the data with the predictions of Mackie and Meares obstruction model. In this model, the diffusion of solvent electrolyte in a resin (polymer) membrane is best described by assuming that the sites occupied by the polymer are permanently unavailable to the ions or to the solvent. Thus, the diffusion of the ions or solvent molecules occurs through the unoccupied sites by polymer chains which imposes a tortuosity in the path length of molecules in motion and expressed as[87,88]:

$$\frac{D_g}{D_o} = \left(\frac{1-\varphi}{1+\varphi}\right)^2 \tag{4}$$

where D_g and D_o are the diffusion coefficients of the ions or solvent molecules in the gel and bulk state, respectively, and φ is the volume fraction of the polymer network. If the number density of the charge-carriers does not change then an equivalent expression in terms of ionic conductivity is described as:

$$\frac{\sigma_g}{\sigma_o} = \left(\frac{1-\varphi}{1+\varphi}\right)^2 \tag{5}$$

where σ_g and σ_o are the ionic conductivities of the ions or solvent molecules in the gel and bulk state, respectively. In Figure 12, Mackie and Meares prediction agrees fairly well for

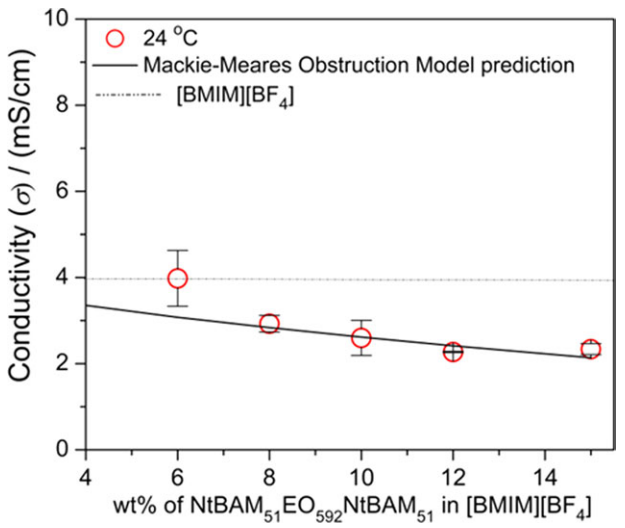

Figure 12. Ionic conductivity (σ) as a function of concentration for $NtBAM_{51}EO_{592}NtBAM_{51}$/[BMIM][$BF_4$] system at 24°C. Error bars in the plot represent standard error of σ for three independent experiments. [Color figure can be viewed in the online issue, which is available at wileyonlinelibrary.com.]

concentrations above 6 wt % where we have fully-developed network structures in the ion-gels.

CONCLUSIONS

In this article, we describe a new set of ion-gels of [BMIM][BF_4] prepared via self-assembly of poly(*N-tert*-butylacrylamide-*b*-ethyleneoxide-*b*-*N-tert*-butylacrylamide) triblock copolymer. At moderately low concentrations of 6 wt %, we demonstrate the formation of strong and thermoreversible ion-gel with high gelation temperature (T_{gel} ~45°C) and ionic conductivities similar to bulk [BMIM][BF_4]. The parameters such as copolymer concentration and solvophobic block length can be easily varied to tune the mechanical and conductivity properties to meet the design specific criteria for various electrochemical applications. Using this block copolymer approach is a better strategy to prepare ion gels with optimal mechanical properties and conductivity compared to bulk [BMIM][BF_4]. Our work in contrast to previous reports where chemical gels are prepared at much higher polymer concentrations using the same IL in which the conductivity of [BMIM][BF_4] is compromised to attain decent mechanical properties for the bulk [BMIM][BF_4]. The IL gels of [BMIM][BF_4] obtained via self-assembly of triblock copolymer is an alternative and attractive way for development of novel solid-state electrolytes and offer exciting possibilities of their application in electrochemical devices including Li-ion batteries.

ACKNOWLEDGEMENTS

Financial support was provided by the University of Connecticut new-faculty start up funds, the American Chemical Society/Petroleum Research Fund (PRF 50863-ND7), and Department of Energy Sustainable Energy grant to the Center for Clean Energy Engineering at University of Connecticut (PE 06302011). Central instrumentation facilities in the Institute of Materials Science and Chemistry Department at University of Connecticut are acknowledged. The authors acknowledge fruitful discussions with Prof. Montgomery T. Shaw. The authors also acknowledge Prof. Steven A. Boggs for helping with the conductivity measurements and fruitful discussions.

REFERENCES

1. Tarascon, J. M.; Armand, M. *Nature* **2001**, *414*, 359.
2. Croce, F.; Appetecchi, G. B.; Persi, L.; Scrosati, B. *Nature* **1998**, *394*, 456.
3. MacFarlane, D. R.; Huang, J. H.; Forsyth, M. *Nature* **1999**, *402*, 792.
4. Gadjourova, Z.; Andreev, Y. G.; Tunstall, D. P.; Bruce, P. G. *Nature* **2001**, *412*, 520.
5. Alarco, P. J.; Abu-Lebdeh, Y.; Abouimrane, A.; Armand, M. *Nat. Mater.* **2004**, *3*, 476.
6. Gray, F. M. Polymer electrolytes. The Royal Society of Chemistry: Cambridge, **1997**.
7. Susan, M. A.; Kaneko, T.; Noda, A.; Watanabe, M. *J. Am. Chem. Soc.* **2005**, *127*, 4976.
8. Christie, A. M.; Lilley, S. J.; Staunton, E.; Andreev, Y. G.; Bruce, P. G. *Nature* **2005**, *433*, 50.
9. Murata, K.; Izuchi, S.; Yoshihisa, Y. *Electrochim. Acta* **2000**, *45*, 1501.
10. Ramesh, S.; Arof, A. K. *Mater. Sci. Eng. B* **2001**, *85*, 11.
11. Chung, S. H.; Heitjans, P.; Winter, R.; Bzaucha, W.; Florjanczyk, Z.; Onoda, Y. *Solid State Ionics* **1998**, *112*, 153.
12. Goodenough, J. B.; Kim, Y. *Chem. Mater.* **2010**, *22*, 587.
13. Xu, K. *Chem. Rev.* **2004**, *104*, 4303.
14. Armand, M.; Endres, F.; MacFarlane, D. R.; Ohno, H.; Scrosati, B. *Nat. Mater.* **2009**, *8*, 621.
15. Garcia, B.; Lavallee, S.; Perron, G.; Michot, C.; Armand, M. *Electrochim. Acta* **2004**, *49*, 4583.
16. Seki, S.; Kobayashi, Y.; Miyashiro, H.; Ohno, Y.; Usami, A.; Mita, Y.; Kihira, N.; Watanabe, M.; Terada, N. *J. Phys. Chem. B* **2006**, *110*, 10228.
17. Welton, T. *Chem. Rev.* **1999**, *99*, 2071.
18. Seddon, K. R. *Nat. Mater.* **2003**, *2*, 363.
19. Plechkova, N. V.; Seddon, K. R. *Chem. Soc. Rev.* **2008**, *37*, 123.
20. Wilkes, J. S. *Green Chem.* **2002**, *4*, 73.
21. Deetlefs, M.; Seddon, K. R. *Chim. Oggi-Chem. Today* **2006**, *24*, 16.
22. Lu, J.; Yan, F.; Texter, J. *Prog. Polym. Sci.* **2009**, *34*, 431.
23. Lodge, T. P. *Science* **2008**, *321*, 50.
24. He, Y.; Boswell Paul, G.; Buhlmann, P.; Lodge Timothy, P. *J. Phys. Chem. B* **2007**, *111*, 4645.
25. He, Y.; Lodge, T. P. *Chem. Commun.* **2007**, 2732.
26. Carlin, R. T.; Fuller, J. *Chem. Commun.* **1997**, 1345.
27. Fuller, J.; Breda, A. C.; Carlin, R. T. *J. Electroanal. Chem.* **1998**, *459*, 29.
28. He, Y.; Lodge, T. P. *Macromolecules* **2008**, *41*, 167.
29. Washiro, S.; Yoshizawa, M.; Nakajima, H.; Ohno, H. *Polymer* **2004**, *45*, 1577.
30. Fuller, J.; Breda, A. C.; Carlin, R. T. *J. Electrochem. Soc.* **1997**, *144*, L67.
31. Wang, P.; Zakeeruddin, S. M.; Comte, P.; Exnar, I.; Gratzel, M. *J. Am. Chem. Soc.* **2003**, *125*, 1166.
32. Chen, Z. G.; Li, F. Y.; Yang, H.; Yi, T.; Huang, C. H. *ChemPhysChem* **2007**, *8*, 1293.
33. Fukushima, T.; Kosaka, A.; Ishimura, Y.; Yamamoto, T.; Takigawa, T.; Ishii, N.; Aida, T. *Science* **2003**, *300*, 2072.
34. Mukai, K.; Asaka, K.; Kiyohara, K.; Sugino, T.; Takeuchi, I.; Fukushima, T.; Aida, T. *Electrochim. Acta* **2008**, *53*, 5555.
35. Aida, T.; Fukushima, T. *Philos. Trans. R. Soc., A* **2007**, *365*, 1539.
36. Hanabusa, K.; Fukui, H.; Suzuki, M.; Shirai, H. *Langmuir* **2005**, *21*, 10383.
37. Ikeda, A.; Sonoda, K.; Ayabe, M.; Tamaru, S.-I.; Nakashima, T.; Kimizuka, N.; Shinkai, S. *Chem. Lett.* **2001**, *11*, 1154.
38. Ribot, J. C.; Guerrero-Sanchez, C.; Hoogenboom, R.; Schubert, U. S. *Chem. Commun.* **2010**, *46*, 6971.

39. Ribot, J. C.; Guerrero-Sanchez, C.; Hoogenboom, R.; Schubert, U. S. *J. Mater. Chem.* **2010**, *20*, 8279.
40. Shin, J.-H.; Henderson, W. A.; Passerini, S. *Electrochem. Commun.* **2003**, *5*, 1016.
41. Boswell, P. G.; Lugert, E. C.; Rabai, J.; Amin, E. A.; Buhlmann, P. *J. Am. Chem. Soc.* **2005**, *127*, 16976.
42. Cho, J. H.; Lee, J.; Xia, Y.; Kim, B.; He, Y.; Renn, M. J.; Lodge, T. P.; Frisbie, C. D. *Nat. Mater.* **2008**, *7*, 900.
43. Lu, W.; Fadeev, A. G.; Qi, B. H.; Smela, E.; Mattes, B. R.; Ding, J.; Spinks, G. M.; Mazurkiewicz, J.; Zhou, D. Z.; Wallace, G. G.; MacFarlane, D. R.; Forsyth, S. A.; Forsyth, M. *Science* **2002**, *297*, 983.
44. Lee, J.; Panzer, M. J.; He, Y.; Lodge, T. P.; Frisbie, C. D. *J. Am. Chem. Soc.* **2007**, *129*, 4532.
45. Huang, J.; Riisager, A.; Wasserscheid, P.; Fehrmann, R. *Chem. Commun.* **2006**, 4027.
46. Fukushima, T.; Asaka, K.; Kosaka, A.; Aida, T. *Angew. Chem. Int. Ed.* **2005**, *44*, 2410.
47. Zhang, S.; Lee, K. H.; Frisbie, C. D.; Lodge, T. P. *Macromolecules* **2011**, *44*, 940.
48. Markevich, E.; Baranchugov, V.; Aurbach, D. *Electrochem. Commun.* **2006**, *8*, 1331.
49. Lewandowski, A.; Swiderska-Mocek, A. *J. Power Sources* **2009**, *194*, 601.
50. Galinski, M.; Lewandowski, A.; Stepniak, I. *Electrochim. Acta* **2006**, *51*, 5567.
51. Tang, Z. L.; Qi, L.; Gao, G. T. *Polym. Adv. Technol.* **2010**, *21*, 153.
52. Lai, J. T.; Filla, D.; Shea, R. *Macromolecules* **2002**, *35*, 6754.
53. Tokuda, H.; Tsuzuki, S.; Susan, M.; Hayamizu, K.; Watanabe, M. *J. Phys. Chem. B* **2006**, *110*, 19593.
54. Triolo, A.; Russina, O.; Keiderling, U.; Kohlbrecher, J. *J. Phys. Chem. B* **2006**, *110*, 1513.
55. Lee, H. N.; Lodge, T. P. *J. Phys. Chem. Lett.* **2010**, *1*, 1962.
56. Sharma, N.; Kasi, R. M. *Soft Matter* **2009**, *5*, 1483.
57. Sharma, N.; Kasi, R. M. *Langmuir* **2010**, *26*, 7418.
58. Brandrup, J.; Immergut, E. H. Eds. Polymer Handbook, 4th ed., John Wiley & Sons, **1998**.
59. De Lambert, B.; Charreyre, M.-T.; Chaix, C.; Pichot, C. *Polymer* **2005**, *46*, 623.
60. de Lambert, B.; Charreyre, M.-T.; Chaix, C.; Pichot, C. *Polymer* **2007**, *48*, 437.
61. Larson, R. G. The Structure and Rheology of Complex Fluids; Oxford University Press: New York, **1999**.
62. Chambon, F.; Winter, H. H. *J. Rheol.* **1987**, *31*, 683.
63. Hess, W.; Vilgis, T. A.; Winter, H. H. *Macromolecules* **1988**, *21*, 2536.
64. Te Nijenhuis, K.; Winter, H. H. *Macromolecules* **1989**, *22*, 411.
65. Valles, E. M.; Carella, J. M.; Winter, H. H.; Baumgaertel, M. *Rheol. Acta* **1990**, *29*, 535.
66. Jeong, B.; Bae, Y. H.; Kim, S. W. *Macromolecules* **1999**, *32*, 7064.
67. Annable, T.; Buscall, R.; Ettelaie, R.; Whittlestone, D. *J. Rheol.* **1993**, *37*, 695.
68. Drzal, P. L.; Shull, K. R. *Macromolecules* **2003**, *36*, 2000.
69. Rossmurphy, S. B.; Shatwell, K. P. *Biorheology* **1993**, *30*, 217.
70. Rossmurphy, S. B. *J. Rheol.* **1995**, *39*, 1451.
71. Aamer, K. A.; Sardinha, H.; Bhatia, S. R.; Tew, G. N. *Biomaterials* **2004**, *25*, 1087.
72. de Gennes, P. G. Scaling Concepts in Polymer Physics; Cornell University Press: Ithaca, NY, **1979**.
73. Doi, M.; Edwards, S. F. The Theory of Polymer Dynamics; Clarendon Press: Oxford, U.K., **1986**.
74. Groot, R. D.; Agterof, W. G. M. *Macromolecules* **1995**, *28*, 6284.
75. Cates, M. E.; Candau, S. J. *J. Phys. Condens. Matter* **1990**, *2*, 6869.
76. Rubinstein, M.; Semenov, A. N. *Macromolecules* **1998**, *31*, 1386.
77. Li, L.; Thangamathesvaran, P. M.; Yue, C. Y.; Tam, K. C.; Hu, X.; Lam, Y. C. *Langmuir* **2001**, *17*, 8062.
78. Qian, X. M.; Gu, N. Y.; Cheng, Z. L.; Yang, X. R.; Wang, E. K.; Dong, S. J. *J. Solid State Electrochem.* **2001**, *6*, 8.
79. Bagdassarov, N.; Freiheit, H. C.; Putnis, A. *Solid State Ionics* **2001**, *143*, 285.
80. Ramesh, S.; Wong, K. C. *Ionics* **2009**, *15*, 249.
81. Agrawal, R. C.; Pandey, G. P. *J. Phys. D: Appl. Phys.* **2008**, *41*, 1.
82. Walden, P. Z. *Phys. Chem.* **1906**, *55*, 207.
83. Hoarfrost, M. L.; Segalman, R. A. *Macromolecules* **2011**, *44*, 5281.
84. Masaro, L.; Zhu, X. X. *Prog. Polym. Sci.* **1999**, *24*, 731.
85. Tokuda, H.; Hayamizu, K.; Ishii, K.; Abu Bin Hasan Susan, M.; Watanabe, M. *J. Phys. Chem. B* **2004**, *108*, 16593.
86. Ueki, T.; Watanabe, M. *Macromolecules* **2008**, *41*, 3739.
87. Mackie, J. S.; Meares, P. *Proc. R. Soc. London A*, **1955**, *232*, 498.
88. Amsden, B. *Macromolecules* **1998**, *31*, 8382.